Combust. Sci. and Tech., 1998, Vol. 134, pp. 183–200
Reprints available directly from the publisher
Photocopying permitted by license only

In Situ Processing of Ferroelectric Materials from Lead Waste Streams by Injection of Gas Phase Titanium Precursors: Laser Induced Fluorescence and X-ray Diffraction Measurements

P. BISWAS[a,*], G. YANG[a] and M. R. ZACHARIAH[b]

[a] *Aerosol and Air Quality Research Laboratory, Environmental, Engineering and Science Division, University of Cincinnati, Cincinnati, Ohio 45221-0071;*
[b] *Process Measurement Division, Chemical Sciences and Technology Laboratory, National Institute of Standards and Technology, Gaithersburg, MD 20899*

(Received 2 March 1998)

Several industrial process exhaust gas streams contain enriched toxic metal species such as lead and cadmium. Gas phase sorbent precursor techniques have been developed to effectively capture these toxic metal species. This methodology is further extended to not only capture the toxic metal species, but produce useful materials. Injection of gas phase titanium precursors to reactively capture the lead species is proposed for the processing of ferroelectric lead titanate materials in enriched lead exhaust streams. Conditions to produce lead titanate in high temperature systems are established. Diagnostic techniques such as X-ray diffraction and laser induced fluorescence spectroscopy are used to determine optimal conditions to not only capture the lead species but also produce perovskite structured lead titanate. Such approaches can be extended to real combustor exhaust streams with high toxic metal concentrations such as lead smelters for effective environmental control and production of novel materials.

Keywords: Air toxics; sorbents; ferroelectric; aerosol; lead; titania

INTRODUCTION

Lead has been used for a number of different applications for thousands of years, its use increasing significantly after the Industrial Revolution. Human

---

*Corresponding author. E-mail: pratim.biswas@uc.edu

activities such as extensive mining, smelting, use in acid batteries, synthesis of tetra alkyl leads and lead paints and as an additive in combustion fuels have resulted in extensive releases into the environment. Though its use in automobile fuels has been gradually phased out since 1970s in the US, it remains to be used in production of various consumer and commercial goods (batteries, lead solders in the microelectronics industry, ceramics, crystal manufacture, paints, smelting and remediation, cathode ray tube protection, ammunitions, radioactive shields, alloys) (Paff and Bosilovich, 1995). Several lead processing systems such as blast furnaces and smelting furnaces operate at high temperatures and the lead species could be potentially entrained in the gases (Clevenger *et al.*, 1991; Trepka, 1997). In high temperature processes exhaust streams, the metallic species are typically concentrated in the submicrometer size ranges and are difficult to capture in particulate control devices (Linak and Wendt, 1993; Lin and Biswas, 1994). Several sorbent methodologies have been proposed for the capture of lead species (Uberoi and Shadman, 1991; Scotto *et al.*, 1992; Ho *et al.*, 1992; Owens and Biswas, 1996a, 1996b). These studies have indicated that lead species can be effectively captured and converted to an environmentally benign form. Combustion systems are also being used to produce a host of materials for a wide variety of applications (such as silica, carbon black, titania). Gas phase combustion synthesis is a method to produce large quantities of materials with controllable morphologies and chemical composition. Specifically, flame reactors offer an effective route in processing of nanostructured materials (Zachariah *et al.*, 1996; Yang *et al.*, 1996). Several combustion exhausts contain high concentrations of lead, such as lead smelting operations. A novel methodology would be to engineer these processes to convert the lead in these exhausts into useful materials.

Lead titanate is a ferroelectric material that has been receiving attention in piezoelectric, pyroelectric, optical and memory devices due to their high curie temperature and low dielectric constant (Huang *et al.*, 1997; Ichinose and Kimura, 1992). Lead titanate has a perovskite structure and shows a cubic to tetragonal phase transition at the curie temperature (490°C); above this temperature it has a cubic structure, and no permanent electrical dipole moment is observable. Below the curie temperature, it is tetragonal and has a permanent electrical dipole moment resulting in ferroelectricity. Several processing routes have been used to synthesize these ferroelectric materials such as solid state reactions, sol-gel techniques, CVD, rf sputtering, magnetron sputtering and flame assisted deposition (Kumar *et al.*, 1996; Polli and Lange, 1995; Weidmann *et al.*, 1995).

In situ measurements for investigating the gas phase species' concentrations, temperature field, and particle size distributions can lead to a better understanding of the underlying chemical/transport phenomena. While conventional diagnostic tools such as thermocouples and mass/particle sampling probes have been used in the past, laser based diagnostics offer non-intrusive, sensitive techniques for such measurements. Light scattering has been used extensively for measurement of particle size and number distributions in both aerosol and combustion research applications (for example, see Zachariah *et al.*, 1989; Biswas, 1993). Laser induced fluorescence (LIF) has been used extensively for gas phase concentration measurements in combustion environments (Eckbreth, 1988). This technique is only recently being exploited in gas-particle conversion systems (Zachariah and Burgess, 1994; McMillin *et al.*, 1996; Biswas and Zachariah, 1997). This is particularly important as the final product composition has to be controlled so that useful materials are produced.

In this paper, we report the use of vapor phase titanium precursors in simulated gas streams carrying lead species vapors to react with the titanium precursor to form ferroelectric lead titanate compounds. Unlike the sorbent control methodologies (Owens and Biswas, 1996a and Biswas and Zachariah, 1997), the objective is not only to capture the lead species, but to also tailor the precursor injection conditions to produce useful ferroelectric materials. As the final composition of the produced powders is critically important, the use of on line diagnostics (laser induced fluorescence spectroscopy) and X-ray diffraction techniques will be discussed in the engineering of the proposed methodology.

EXPERIMENTAL SYSTEM AND PLAN

The schematic diagram of the experimental system is shown in Figure 1. Two different systems were used: a burner configuration and a furnace configuration. The first set of experiments were carried out in a multi-port diffusion flame burner (Lin *et al.*, 1992; Yang *et al.*, 1996). Precursors are entrained in an air stream and introduced into the flame through the center port of the burner, the methane as the fuel is introduced *via* the second port. To achieve a desired (high) temperature flame environment, oxygen is optionally introduced into the third port. Vapors of organo-titanium and lead are introduced by nebulizing (Collision Nebulizer CN-25, BGI Inc.) and bubbling (7532 Midget Bubbler, ACE Glass Inc.) air through titanium isopropoxide and tetraethyl lead precursor solutions (Aldrich Inc.)

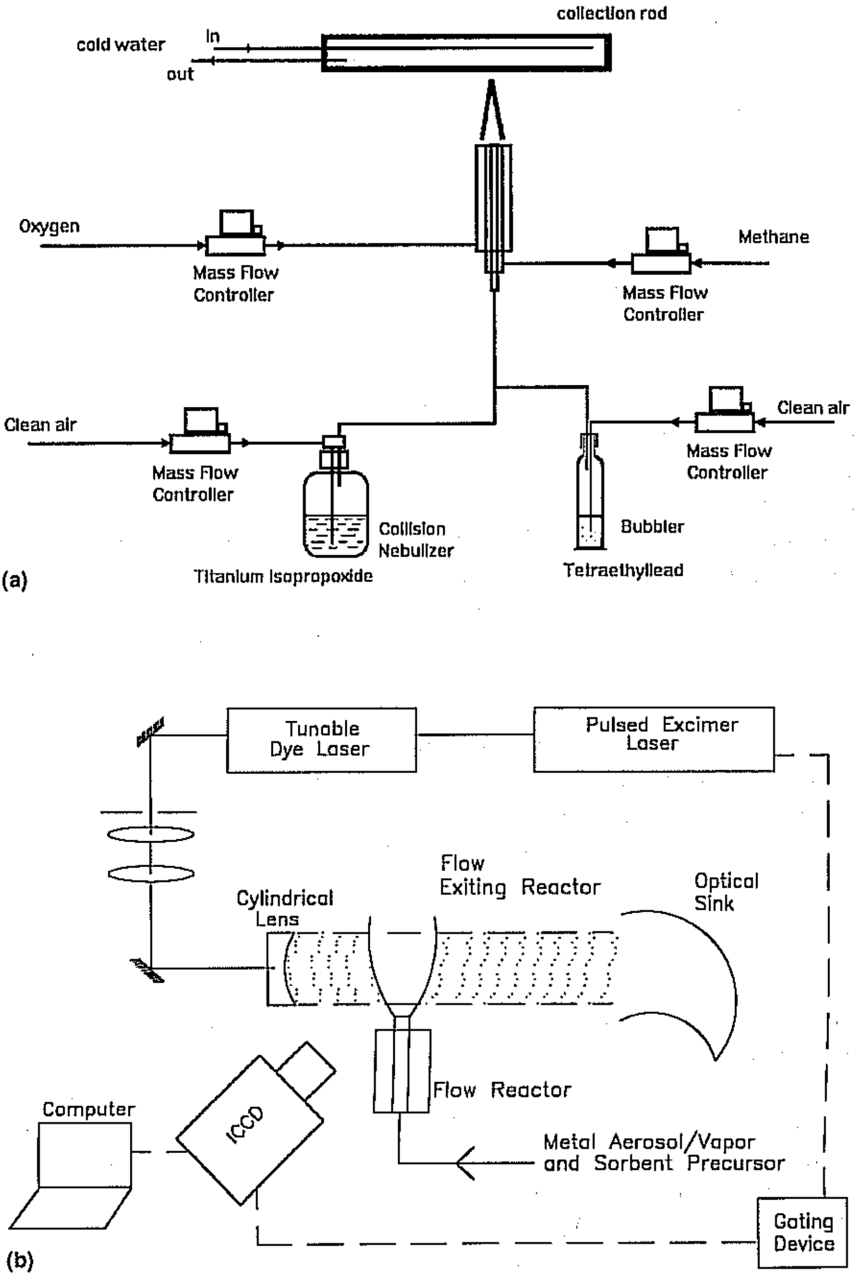

FIGURE 1 Schematic diagram of experimental system. (a) Diffusion flame aerosol reactor for powder collection, (b) System for performing Laser Induced Fluorescence Measurements.

respectively. A nebulizer was used to feed the titanium precursor due to its lower volatility. Calibration experiments were carried out to establish the feed rates of the precursors as a function of the carrier gas flow rates. The particles that were produced under the different operating conditions (Tab. I) were collected on a cooled, collection rod similar to that described in Yang *et al.* (1996). To obtain the characteristics of the reacting system at different temperatures, the gases were cooled down rapidly and the particles were collected on the rod by thermophoretic deposition. The collected particles were analysed by X-ray diffraction (XRD) to establish their composition.

The first set of experiments described above provided the optimal conditions for the capture of the toxic lead species and formation of the perovskite lead titanate. The objective was then to confirm the consumption of the gas phase lead oxide using laser induced fluorescence spectroscopy. The next set of experiments were carried out using a water cooled, premixed burner mounted on a vertical translation stage (McMillin *et al.*, 1996). Methane – oxygen flames with appropriate dilution using nitrogen was used to obtain a stable premixed flame. The lead precursor (tetraethyl lead) was entrained in an argon stream by bubbling and mixing with the fuel-oxidant mixture prior to introduction into the flame. This system was used to elucidate PbO spectroscopy and obtain the laser induced fluorescence characteristics. Experiments were then conducted with a co-feed of the titanium precursor (titanium isopropoxide) also entrained in an argon stream by vapor saturation. The second set of experiments were conducted by using a furnace reactor similar to that described in Biswas and Zachariah (1997), with measurements made at the exit of the reactor. The lead and titanium precursor were premixed with oxygen and nitrogen and inlet into the furnace reactor.

The laser excitation source for the experiments was an XeCl excimer-pumped dye laser, operating at 10 Hz with a 30 ns pulse duration and approximately 5 mJ pulse energy, and 0.2 cm^{-1} bandwidth. For the initial spectroscopy measurements, the cylindrical beam was directed through the flame region and the fluorescent intensity monitored as a function of the incident wavelength (from 565–572 nm). A PMT was used to detect the fluorescent light intensities. To minimize contributions from scattering, a long pass filter (OG-590, Schott glass filter) was used to block light of wavelength less than 590 nm from being detected by the PMT. After selection of an excitation frequency (details in PbO spectroscopy section), a cylindrical and spherical lens combination was used to obtain a sheet beam which was directed over the measurement region as shown in Figure 1b. The

TABLE I List of flame experiments performed

Case No	Flow rate (liter/min.)				Molar ratio Ti : Pb	Peak flame temp.°C	Powder phase composition	Color of powder
	CH_4	O_2	Air (Pb)	Air (Ti)				
1	0.40	0.0	0.0	5.0	Ti only	910	anatase + rutile	white
2	0.40	0.0	5.0	0.0	Pb only	910	Massicot + unknown	brown
3a	0.40	0.0	2.0	3.1	1	910	amorphous	white
3b	post annealing of sample 3a in open air at 800 C for 20 min						$PbTi_3O_7$ crystal	yellow
4	0.55	0.0	1.3	2.7	1	1100	$PbTiO_3$ crystal	white
5	0.55	1.0	1.3	2.7	1	1510	anat. + rut. + mass. + unkn.	yellow
6	0.55	0.0	1.0	2.7	1.2	1100	rutile + $PbTiO_3$	white
7	0.55	0.0	1.0	3.0	1.4	1100	anatase + rutile + amorph.	white
8	0.55	0.0	1.0	2.3	0.8	1100	Massicot + $PbTiO_3$	yellow
9	0.55	0.0	1.0	1.8	0.6	1100	Massicot + $PbTiO_3$	yellow

laser energy and its spatial distribution were monitored during the experiments by directing a 5% reflection of the laser sheet onto a dye cell and recording the intensity with a video CCD camera and frame grabber computer board. A line filter (Corion P10–530 nm) was used for the light scattering measurements (no fluorescence at 530 nm).

The images obtained were averaged over 250 laser shots to improve the signal to noise ratio, and were spatially averaged 2×2 pixels which is the effective resolution of the intensifier. All the image intensities were then corrected for camera dark background, flatfield uniform response of the camera and collection lens, and laser energy and spatial distribution. The fluorescence images were also corrected for laser induced particle incandesence and scattering by subtracting images obtained with the laser detuned from the absorption transition. The flatfield correction was obtained by imaging uniform light from a standard, diffuse tungsten lamp, through the appropriate spectral filters for fluorescence or particle scattering. As mentioned above, the video CCD images of laser induced fluorescence from a static cell of dilute Rhodamine 590 dye in methanol were used to normalize the laser energy and vertical spatial distribution in the corrected images. The laser profile images were re-mapped from the video CCD to the intensified CCD coordinates based on images obtained with the laser sheet masked.

RESULTS AND DISCUSSION

The results are discussed in the following sections. First, a discussion of the detailed characterization of the resultant powders, and identifying the conditions to both capture the lead species, and produce the perovskite phase of lead titanate (an useful ferroelectric material) is provided. This is followed by a brief discussion of the spectroscopy of gas phase lead oxide and selection of the excitation wavelength for performing the laser induced fluorescence measurements. This is followed by reporting results of a LIF measurement to elucidate the mechanistic behavior of the reacting system.

Capture of Lead Species and Characterization of Resultant Particles

A sequence of experiments were performed to establish the relation between titanium precursor injection rate and temperature to the lead levels in the gas stream with the objective of obtaining lead titanate with a perovskite structure. First, a detailed characterization of the powders for different operating conditions is carried out (Tab. I), and this is followed by a laser induced fluorescence study of the reacting system.

The first set of experiments (Cases 1 through 4) were carried out at different operating flame temperatures, controlled by varying the air fuel ratio. The first set of experiments were carried out with a "titanium only" (Case 1) and a "lead only" (Case 2) feed to establish the characteristics of the resultant particles. The X-ray diffraction patterns are shown in Figure 2. For Case 1, the anatase phase was predominantly obtained, with a small

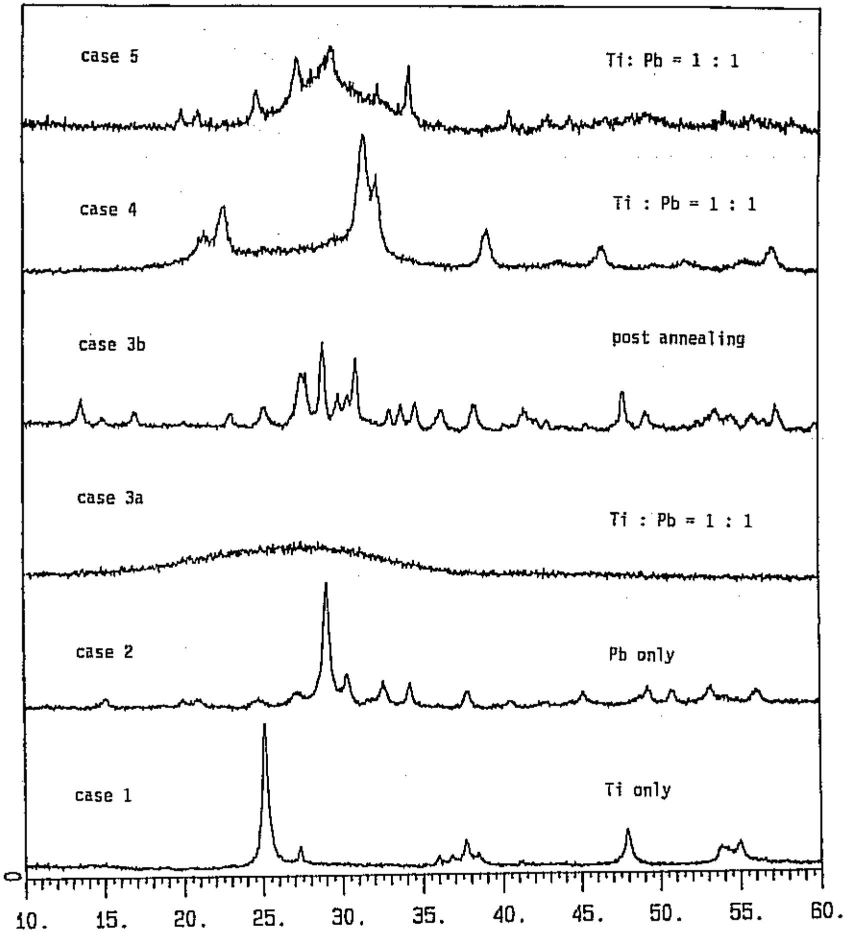

FIGURE 2 X-ray diffraction patterns for powders generated under conditions of Cases 1 through 5.

percentage of the rutile phase. A detailed study of the crystal nucleation and phase transformations were discussed in an earlier paper by Yang *et al.* (1996), and the reader is referred to that paper for details. For Case 2, reddish brown lead oxide particles were obtained consisting primarily of the massicot phase. This is similar to the furnace reactor experiments performed by Wu (1996), however, there are some other forms of the lead species (peaks could not be identified as per the current JCPD database). These peaks were also observed for the high temperature experiments (Case 5). The next experiment (Case 3a) performed was with a ratio of Ti : Pb of 1 : 1, at the same fuel-air ratio, thus maintaining the temperature same as in Cases 1 and 2. As the precursor concentrations are low compared to the fuel concentration, the heat release due to chemical reactions did not alter the system temperatures. A pure white powder was collected which was found to be amorphous (Fig. 2). Thus the crystallization of neither titania nor lead oxide particles took place, and the intermediate monomer species (TiO and PbO) reacted to form an amorphous solid-state complex. Similar results have been obtained for lead-silicon systems, wherein an amorphous lead silicate compound was obtained (Owens and Biswas, 1996b; Biswas and Zachariah, 1997). The residence time – temperature conditions establish if the crystal forms of lead titanate (perovskite structure) are obtained. The residence time is not sufficient to form the lead titanate crystals under the conditions of these experiments. The collected particles were then annealed in air at 800°C for approximately 20 minutes, and the crystalline $PbTi_3O_7$ compound was obtained. Though the ratio of the Ti/Pb is 1 in the original mix, some of the lead volatilizes resulting in $PbTi_3O_7$ ($Ti/Pb = 3$) as the only observed compound.

The above experimental results indicate that the environmental goals have been met, as the lead is effectively reacted with the injected material (analog of the sorbent, Biswas and Owens, 1996a). Though a crystalline material could be produced by post annealing, the goal from a materials processing viewpoint is to produce the final product powder (perovskite lead titanate) in a single step. Thus, to facilitate *in situ* annealing, the next experiment (Case 4) was carried out at a higher temperature (by reducing the air flow rate, which also increased the residence time). The XRD patterns of the as collected powders indicated that the crystalline forms of lead titanate could be readily produced. No lead oxide particles were observed. These results, though from laboratory scale systems, clearly indicate that the lead species was successfully immobilized and reacted with the titanium species to form a ferroelectric material, thus demonstrating a potentially innovative environmentally benign technology. To further examine the role of temperature, an experiment was conducted at a temperature of 1510°C (Case 5), and in this case the lead-titanium complex was not formed. XRD patterns indicate that the massicot phase of lead oxide and the anatase and rutile phases of titania were obtained. This is consistent with the equilibrium predictions of Owens and Biswas (1995) and similar to the high temperature experiments of lead and silica species reported by Biswas and Zachariah (1997). At high temperatures, the lead-titanium complex is not stable, and on quenching (collection rod) the vapors nucleate separately to form titania and lead oxide particles. The titania particles are stable at the high temperatures (Yang and Biswas, 1997; similar to silica particles, Biswas and Zachariah, 1997), however, they do not have a chemical affinity for lead oxide vapor at very high temperatures (lead titanate is not the favored compound formed).

The next set (Cases 6 through 9) of experiments were performed at a fixed temperature of 1100°C by varying the Ti/Pb ratio. The XRD patterns are illustrated in Figure 3. The Ti : Pb ratio is increased to 1.2 and 1.4 in Cases 6 and 7 respectively. Interesting results are obtained, the excess titanium nucleates to form the crystalline anatase and rutile phases, and majority of the lead is associated with the titanium as an amorphous complex (some crystalline lead titanate was observed in Case 6). This is identical to the results reported by Owens and Biswas (1996b) for a lead-silicon reacting system, with excess silica. As stated earlier, this is acceptable (was even considered desirable) from an environmental standpoint as all the lead species is complexed with the titania. An interesting result is that the rutile phase becomes more predominant, clearly due to doping effects associated with the lead species. Similar results have been reported by other researchers on doping effects (Shannon and Pask, 1965; Suyama and Kato, 1985).

On reducing the Ti : Pb ratio (Cases 8 and 9), there is unreacted lead in the mix, and a combination of lead oxide and crystalline lead titanate is obtained. This is contrary to the excess titanium feed cases (6 and 7) where no crystalline lead titanate was obtained. Thus excess lead in the system results in the formation of the crystalline lead titanate, but not when there is excess titania in the system. One reason for this is due to the higher volatility of the lead species. Thus lead in the system will help in the formation of crystalline lead titanate, but not if there is a deficiency. The presence of the lead oxide is not acceptable from an environmental view point.

PbO Spectroscopy

The theory and application of laser induced fluorescence spectroscopy has been described in detail elsewhere (Eckbreth, 1988). PLIF (Planar Laser

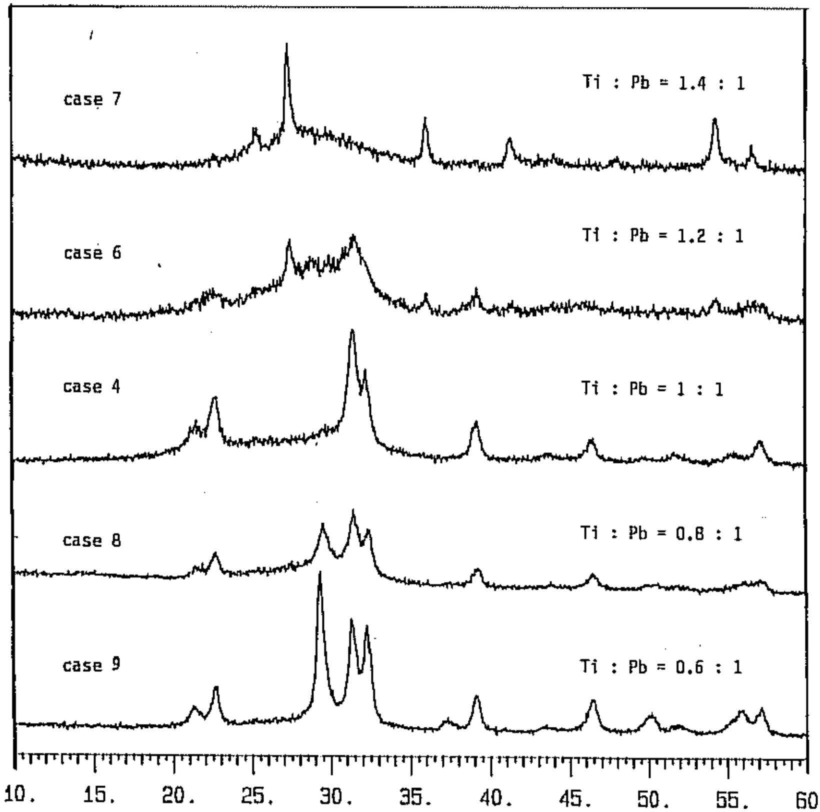

FIGURE 3 X-ray diffraction patterns for powders generated under conditions of Case 4, and Cases 6 through 9.

Induced Fluorescence) is a well established spectroscopic flow diagnostic that is based on the spontaneous radiaitive emission (fluorescence) following absorption of laser photons by a specific molecular species. In a typical PLIF measurement, a thin sheet of frequency tuned pulsed laser light is used as the excitation source and directed through the flow region of interest. The resulting broadband fluorescence from the illuminated region is imaged with a lens onto an intensified charge coupled device (CCD) camera. Through various excitation and detection strategies, the pulse integrated fluorescence signal can be related to the absorbing species concentration (McMillin *et al.*, 1996; Biswas and Zachariah, 1997). The absorbing species côncentration generally requires knowledge of the local collisional quenching rate coefficient and temperature. One strategey that is used is to assume a constant quenching rate (Zachariah and Burgess, 1994; McMillin *et al.*,

1996) and an absorption transition that is insensitive to temperature (discussed later). Using these approximations, the fluorescence signal is a direct representation of the relative PbO(g) concentration in the flame.

There have been several reports on the spectroscopy of lead oxide in the literature. High resolution absorption studies of PbO have been reported by Shawhan and Morgan (1935) and Barrow *et al.* (1961). High resolution emission studies of PbO have been reported by Christy and Blomenthal (1930) and Ram *et al.* (1973). The technique of gas chemiluminescence and laser induced fluorescence have been used by Oldenborg *et al.* (1973) to identify a series of 55 bands in the 450 to 850 nm range. Several new bands of the chemiluminescent spectra of PbO were reported by Linton and Broida (1976), primarily for the $A0^+-X0^+$ transitions. The only study reporting the laser excitation spectrum of PbO was by Brom and Beattie (1980). A flashlamp-pumed tunable dye laser was used to investigate the a-X band system of PbO. Dorko and coworkers (1986) have characterized the chemiluminescence from electronically excited lead oxide. Martin *et al.* (1988) report a high resolution Fourier transform spectroscopy of the PbO molecule and have reported the spectroscopic constants for a variety of transitions.

The partial fluorescence excitation-detection scheme and associated energy level diagram is shown in Figure 4. Represented schematically is the $A^3\Pi\ (0^+) \leftarrow X^1\Sigma^+(0^+)\ (0, 3)$ excitation and the ground level vibration states, $v'' = 0, 1, 2, 3, 4, 5$ and 6. The upward pointing arrow indicates the laser excitation frequency that was tuned to excite transitions from a particular rotational level within the $v'' = 3$ ground state to the $v'' = 0$ level in the excited A state. The downward pointing arrows in the figure depict the radiative (fluorescent) or non-radiative (quenched) decay from the excited state (A) to various lower states. The partial excitation frequency spectrum obtained by scanning the laser from 567.5 nm to 571.5 nm in steps of 0.001 nm is shown in Figure 5. Using the spectroscopic constants reported by Oldenberg *et al.* (1973), the synthetic spectra were calculated for the above mentioned transition, and rotational line assignments made (Fig. 5).

While transition probabilities are relatively independent of rotational state, the population in each rotational state is a function of temperature. Hence the absorption and fluorescence are also a function of temperature, this being related to the fractional population (F_B) of the j^{th} rotational state (Banwell, 1983) being excited

$$F_B = \frac{(2j+1)\exp\left[(-hc/kT)(T_e + G(v) + F(j))\right]}{Q_e Q_v Q_r} \tag{1}$$

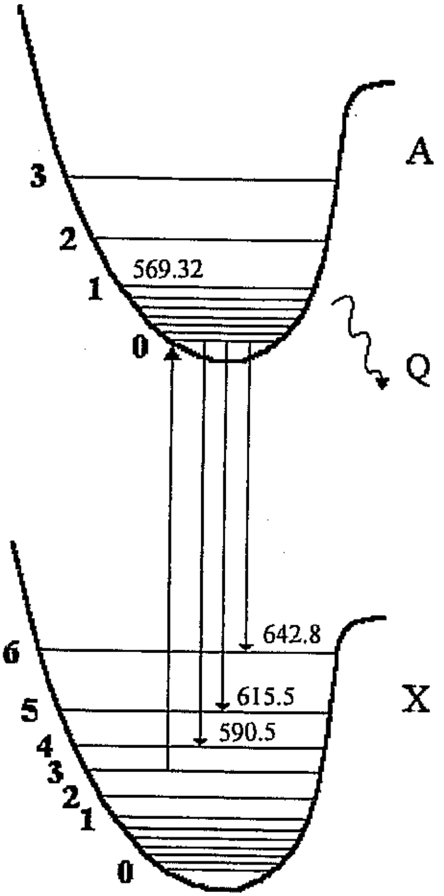

FIGURE 4 Partial energy level diagram for PbO showing the excitation and detection scheme used in this study.

where h is the Planck's constant, c is the velocity of the light, k is the Boltzmann constant, T is the temperature, T_e is electronic energy level, $G(v)$ is the vibrational energy level, $F(j)$ is the rotational energy level, Q_e [$=1$] is the electronic partition function, Q_v[$=1/(1-\exp(-hc\omega_e/kT))$] is the vibrational partition function, ω_e is the vibrational frequency, and Q_r[$=kT/hcB_v$] is the rotational partition function, B_v is a rotational constant. Using equation 1, the computed fractional population, F_B, is plotted as a function of temperature for different rotational states in Figure 6. Over the temperature range of 1800 K to 2400 K, the net population of the $Q(30)$ line (corresponding to a 569.32 nm excitation) varied by only 10% (Fig. 6). Over

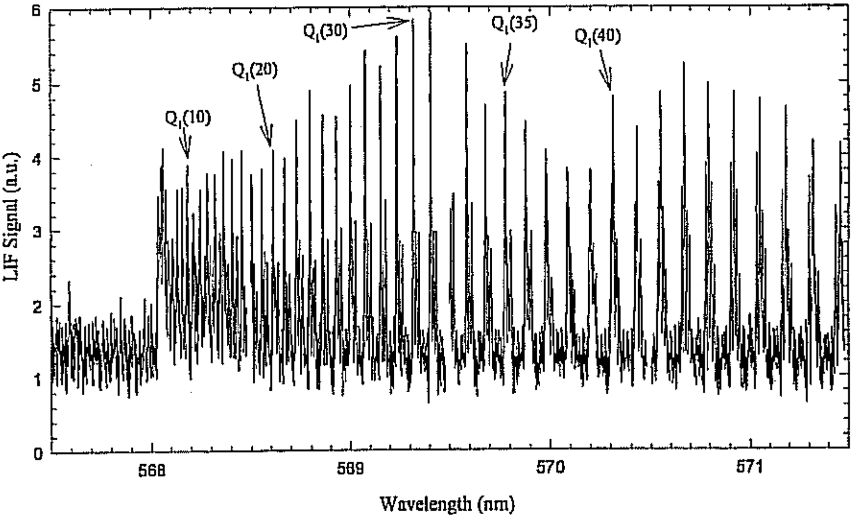

FIGURE 5 Laser excitation spectrum of PbO between 567.5 nm and 571.5 nm established with a resolution of 0.001 nm. Also shown are rotational states for a few lines.

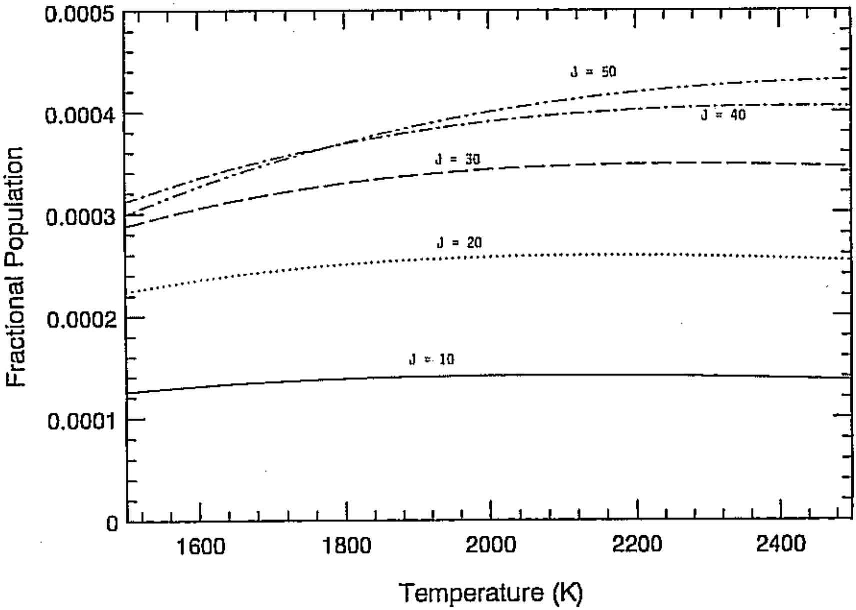

FIGURE 6 Expected temperature dependence of the fluorescence signal based on the variation of the Boltzmann population distribution with temperature.

the temperature range of 1000 K to 1200 K the net population varied by less than 15%.

Laser Induced Fluorescence Measurements

The set of experiments described earlier was useful in establishing conditions that would result in the formation of the lead titanate crystal structure. LIF measurements were used to monitor the reaction of lead species in the system. The results of experiments performed at 1100°C are reported, as this was found to be the optimal condition from the previous experiments (Case 4, Tab. I). The temperature in the LIF measurement zone varied from 1100°C to approximately 707°C, at a distance of 35 mm from the exit of the reactor. The gases at the exit of the reactor were monitored for gas phase lead oxide concentrations. As discussed earlier, an incident wavelength of 569.32 nm was used to obtain the fluorescent signal. The normalized PbO concentrations for a "lead only" and "lead + titanium" feed are plotted in Figure 7. In the lead only feed case, the lead concentration decreases slightly

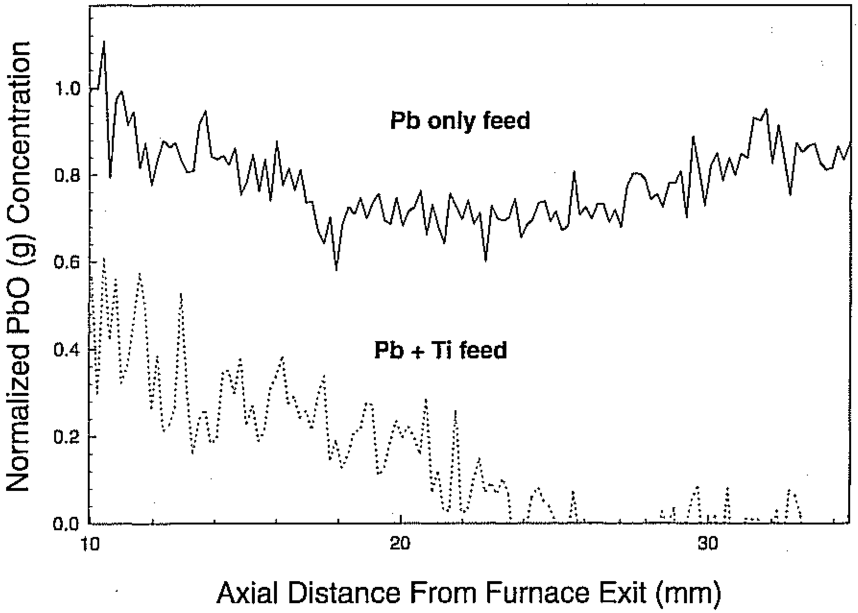

FIGURE 7 Centerline profile of normalized (by concentration at exit of furnace for a lead only feed) PbO(g) concentration and lead + titanium precursor feed at the exit of the furnace reactor as a function of distance (Furnace temperature = 1100°C, Total flow rate of gases = 5.75 lpm at 25°C).

due to the drop in temperature and formation of lead oxide particles (slow rate due to the relatively high temperatures). For the co-feed, the concentration of the PbO(g) species at the outlet of the reactor itself is lower ($x = 10$ mm) due to reaction with the titania particles at the high temperatures inside the furnace (over a short duration). A further drop in the co-feed case is observed, clearly indicating a reactive scavenging of the lead oxide species. The concentration drops off to a very low value, and as the temperatures decreases downstream, the concentration reduces to practically zero. These results clearly confirm the complete reaction of the lead species with the titanium dioxide and no lead oxide vapors are available at cooler downstream sections to nucleate to form lead oxide particles. In comparison to lead–silica reactions, it is noted that titanium precursors are more effective at scavenging lead species (Biswas and Zachariah, 1997).

CONCLUSIONS

The study has illustrated that lead species in a gaseous stream can be reacted with gas phase sorbent precursors to form useful ferroelectric lead titanate materials. Though there is evidence that this process will work for exhausts with lead species vapors (such as lead soldering exhaust streams, smelter furnace exhausts), optimal conditions have to be determined for specific systems by using an approach (with diagnostic tools) outlined in this paper. A detailed laboratory scale study successfully identified conditions for maximizing the production of lead titanate, at the same time minimizing the emission of lead species. *In situ*, planar laser induced fluorescence imaging can provide real time information on the lead–titanium reaction system, and can also be used to establish optimal conditions for capture of lead species.

The potential of *in situ* generated sorbents for metals capture reported earlier is confirmed by the results from this work. A networked agglomerate of titania particles is formed at combustor temperatures. The metallic species undergo various reactions and intermediate oxide species are typically formed in the gas phase. As the sorbent oxide has a high affinity for the metal oxide, these vapors are effectively scavenged, the effectiveness being highest at a lower optimal temperature (encountered as the gases traverse down the combustor). As the metal species vapors are effectively removed, sufficient quantities are not present to nucleate and form the ultrafine mode of the aerosol which is difficult to capture. Relatively low ratios of sorbent to metal have been shown to be effective for high capture efficiencies. Conditions to obtain novel materials with high technology applications as the products have also been established.

Acknowledgements

Partial support was provided by the Chemical Sciences Technology Laboratory, NIST, and the US Department of Energy (Grant DE-FG22-95PC95222). The authors also acknowledge the assistance of Maria Aquino, NIST in conducting some of the experiments.

References

Banwell, C. N. (1983) Introduction to Molecular Spectroscopy, McGraw Hill.

Barrow, R. F., Deutsch, J. L. and Travis, D. N. (1961) *Nature*, **191**, 374.

Biswas, P. (1993) in Aerosol Measurement: Principles, Techniques and Applications, Willeke K. and Baron, P. (Eds.), Chap 32, Van Nostrand, NY.

Biswas, P. and Zachariah, M. R. (1997) *Environ. Sci. Technol.*, **31**, 2455.

Brom, J. M. and Beattie, W. H. (1980). *J. Mol. Spectroscopy*, **81**, 445.

Christy, A. and Blomenthal, S. (1930). *Phys. Rev.*, **35**, 46.

Clevenger, T. E., Slawan, C. and Koirtyohann, S. R. (1991). *Environ. Sci. Technol.*, **25**, 1128.

Dorko, E. A., Glessner, J. W., Ritchey, C. M., Rutger, L. L., Pow, J. J., Brasure, L. D., Duray, J. P. and Snyder, S. R. (1986) *Chem. Physics*, **102**, 349.

Eckbreth, A. C. (1988) Laser Diagnostics for Combustion Temperature and Species, Abacus Press, Cambridge, MA.

Ho, T. C., Chen, C., Hopper, J. R. and Oberacker, D. A. (1992) *Combust. Sci. Technol.*, **85**, 1001.

Huang, H. J., Watari, K. and Sando, M. (1997) *J. Am. Ceramic Soc.*, **80**, 791.

Ichinose, N. and Kimura, M. (1992) *Jpn. J. Appl. Phys.*, **31**, 3033.

Kumar, V., Marimuthu, R. and Patil, S. G. (1996) *J. Am. Ceramic Soc.*, **79**, 2775.

Lin, W. Y., Sethi, V. and Biswas, P. (1992) *Aerosol Sci. Technol.*, **17**, 119.

Lin, W. Y. and Biswas, P. (1994) *Combust. Sci. Technol.*, **101**, 29.

Linak, W. P. and Peterson, T. W. (1986) *24th Combustion (Intl.) Symposium*, 399.

Linak, W. P. and Wendt, J. O. L. (1993) *Prog. Energy Combust. Sci.*, **19**, 145.

Linton, C. and Broida, H. P. (1976) *J. Mol. Spectrosocopy*, **62**, 396.

Martin, F., Bacis, R., Verges, J., Bachar, J. and Rosenwaks, S. (1988) *Spectrochimica Acta*, **44**, 889.

McMillin, B., Biswas, P. and Zachariah, M. R. (1996) *J. Mater. Res.*, **11**, 1552.

Oldenborg, R. C., Dickson, C. R. and Zare, R. N. (1973) *J. Mol. Spectroscopy*, **58**, 283.

Owens, T. M.,Wu, C. Y. and Biswas, P. (1995) *Chem. Engr. Comm.*, **133**, 31.

Owens, T. M. and Biswas, P. (1996a) *Ind. Eng. Chem. Res.*, **35**, 792.

Owens, T. M. and Biswas, P. (1996b) *J. Air Waste Mgmt. Assocm.*, **46**, 530.

Paff, S. W. and Bosilovich, B. E. (1995) *J. of Haz. Materials*, **40**, 139.

Polli, A. D. and Lange, F. F. (1995) *J. Am. Ceramic Soc.*, **78**, 3401.

Ram, R. S., Singh, J. and Upadhya, K. N. (1973) *Spectrosc. Lett.*, **6**, 515.

Scotto, M. V., Peterson, T. W. and Wendt, J. O. L. (1992) *2nd Intl. Congress on Toxic Combustion by Products*, Salt Lake City, UT.

Shannon, J. D. and Pask, J. A. (1965) *J. Am. Ceramic Soc.*, **48**, 391.

Shawhan, E. N. and Morgan, F. (1935) *Phys. Rev.*, **47**, 377.

Suyama, Y. and Kato, A. (1985) *J. Am. Ceramic Soc.*, **68**, 154.

Trepka, M. J. (1997) *Environ. Research*, **72**, 118.

Uberoi, M. and Shadman, F. (1990) *AIChE J.*, **36**, 1433.

Uberoi, M. and Shadman, F. (1991) *Environ. Sci. Technol.*, **25**, 1285.

Wiedmann, I., Choy, K. L. and Derby, B. (1995) In Thin Film Deposition, Ed. Smith, D. L., p. 133, McGraw Hill, NY.

Wu, B., Jaanu, K. K. and Shadman, F. (1995) *Environ. Sci. Technol.*, **29**, 1660.

Wu, C. Y. (1996) "Study of Gas Phase Reactions, Aerosol Formation and Growth Dynamics of Toxic Metals at High Temperatures", Ph.D. Thesis, Chap. 4, Univ. of Cincinnati.

Yang, G., Zhuang, H. and Biswas, P. (1996) *Nano Structured Materials*, **7**, 675.

Yang, G. and Biswas, P. (1997) *Aerosol Sci. Technol.*, **27**, 507.

Zachariah, M. R., Chin, D., Semerjian, H. G. and Katz, J. L. (1989) *Appl. Opt.*, **28**, 530.

Zachariah, M. R. and Burgess, D. R. F. (1994) *J. Aerosol. Sci.*, **25**, 487.

Zachariah, M. R., Shull, R. D., McMillin, B. K. and Biswas, P. (1996) Nanotechnology, Chapter 3, Eds. Chow, G. M. and Gonsalves, K. E., ACS Symposium Series.